Multiple-Input Deep Convolutional Neural Network Model for COVID-19 Forecasting in China

Chiou-Jye Huang [1], Yung-Hsiang Chen [2], Yuxuan Ma [1] and Ping-Huan Kuo [3,*]

[1] School of Electrical Engineering and Automation, Jiangxi University of Science and Technology, Ganzhou, Jiangxi, 341000, China; cjhuang@jxust.edu.cn; 1103552453@qq.com
[2] Department of Mechanical Engineering, National Pingtung University of Science and Technology, Pingtung 91201, Taiwan; yhchen@mail.npust.edu.tw
[3] Computer and Intelligent Robot Program for Bachelor Degree, National Pingtung University, Pingtung 90004, Taiwan; phkuo@mail.nptu.edu.tw
* Correspondence: phkuo@mail.nptu.edu.tw; Tel.: +886-87663800 ext. 32620

Abstract: COVID-19 is spreading all across the globe. Up until March 23, 2020, the confirmed cases in 173 countries and regions of the globe had surpassed 346,000, and more than 14,700 deaths had resulted. The confirmed cases outside of China had also reached over 81,000, with over 3,200 deaths. In this study, a Convolutional Neural Network (CNN) was proposed to analyze and predict the number of confirmed cases. Several cities with the most confirmed cases in China were the focus of this study, and a COVID-19 forecasting model, based on the CNN deep neural network method, was proposed. To compare the overall efficacies of different algorithms, the indicators of mean absolute error and root mean square error were applied in the experiment of this study. The experiment results indicated that compared with other deep learning methods, the CNN model proposed in this study has the greatest prediction efficacy. The feasibility and practicality of the model in predicting the cumulative number of COVID-19 confirmed cases were also verified in this study.

Keywords: Total confirmed forecasting; convolutional neural network; COVID-19

1. Introduction

In early December 2019, the first case of COVID-19 infection was discovered in Wuhan City in China's Hubei Province [1]. In the following weeks, this disease broke out within China and continued to spread extensively in other countries, causing worldwide panic. The pneumonia caused by this novel coronavirus was officially named the Coronavirus disease 2019 (COVID-19) by the World Health Organization (WHO). The 2019 coronavirus epidemic was triggered by the Severe Acute Respiratory Syndrome Coronavirus 2 (SARS-CoV-2), and it has, at the time of writing, spread in over 173 countries, causing more than 15,000 deaths. The epidemic is still spreading, and the WHO has classified the global risk level of the disease as a "pandemic." Currently, the earliest known case symptoms appeared on December 1, 2019, and the first case sought treatment on December 8. On December 26, 2019, Wuhan City Respiratory and Intensive care doctor Zhang Jixian first discovered this pneumonia with unknown cause and suspected that it is an infectious disease. Subsequently, the disease broke out in Wuhan City. On January 20, 2020, Chinese academic Zhong Nanshan publicly announced that the novel coronavirus pneumonia "definitely transmits between people." On January 23, 2020, the Wuhan City Government announced the adoption of lockdown and quarantine measures in the infected areas, which was the first case of lockdown in a major city (with a population of 11 million) in recent public health history. Since January 13, the disease continued to spread to Thailand, Japan, and South Korea. On January 30, three countries outside China were verified as having interpersonal propagation, and the pandemic was thus designated as an international public health emergency event by the WHO.

According to reports on the epidemic, "the propagation speed is faster, and the virus propagation power has increased." Infected people can infect others with the virus while exhibiting no symptoms; and the latency from infection to the presentation of symptoms is as long as 14 days. These characteristics also increase the difficulty of controlling the epidemic. As the epidemic continues, there is also a problem of the global undersupply of surgical masks. Currently, no vaccine and remedy for the novel coronavirus have been discovered. WHO assistant director-general Bruce Aylward stated that Remdesivir is currently the only drug

that is "considered to probably have real efficacy." The China–Japan Friendship Hospital in China and the American National Institute of Allergy and Infectious Diseases are starting to conduct clinical trials for the drug. At present, no sufficient knowledge regarding the disease is known, and key factors, such as virus source, virus birthplace, morbid mechanism, virus pathogenicity, and propagation power are still uncertain. The WHO stated on March 3 that with the novel coronavirus epidemic, the world is in an "unknown state."

Up until March 23, 2020, 345,297 people have been infected with the virus; among these people, 14,765 have died. The several European countries with the most severe epidemics have experienced the maximum increase in confirmed cases in a single day on March 5: cases for Italy increased from 3,089 to 3,858, those for Germany increased from 262 to 482, those for France increased from 285 to 423, and those for the Netherlands increased more than twofold from 38 to 82. In the WHO report on February 26, the numbers of new cases in China and Japan have decreased, but the numbers of new cases in Italy, Iran, and South Korea are still rising. At the time of writing, the numbers of confirmed cases in Germany, France, and Spain have surpassed 1,000.

2. Related Works

Fig. 1 [2] presents the global map of COVID-19 occurrence according to data from the United States' Centers for Disease Control and Prevention. The countries marked with a color are countries with confirmed cases. At present, 173 of the 195 countries in the world have confirmed cases, underscoring the epidemic's astounding speed of propagation from its origin in China's Hubei province. Most scholars have used mathematical models to predict the spread of COVID-19. Roosa et al. [3] used the generalized logistic model, the Richards model, and the sub-epidemic model to establish prediction models for the cumulative numbers of confirmed cases in Guangdong Province and Zhejiang Province. They predicted that, in the next 5 days and 10 days from their time of writing, 65–81 and 44–354 new cases will appear in Guangdong and Zhejiang provinces, respectively. In addition, Liu et al. [4] used mathematical models to simulate the propagation status of COVID-19 in China and noted the importance of the government's policy of limiting public activities and the movement of infected people with no symptoms. Boldog et al. [5] adopted a Time-Dependent Compartmental Model of the Transmission Dynamics to estimate the cumulative number of confirmed cases outside of Hubei Province. Moreover, the Galton–Watson branch was used to analogize virus propagation, thus determining the connectivity and transmissibility between China and the destination country. The disadvantage of this method is that the uncertainty regarding the efficacy of control measures against the disease results in difficulties in predicting the development trajectories of the disease. By comparison, Al-Qaness et al. [6] adopted the adaptive neuro-fuzzy inference system (ANFIS), an improvement from flower pollination algorithm and salp swarm algorithm, to predict the number of confirmed cases in the next 10 days. The comparison with the ANFIS optimized with GA, PSO, ABC, and FPA indicated that the accuracy of the FPASSA-ANFIS model reached 0.97, and the predicted average increase in numbers of new cases in the next 10 days was 10% more than the number of present cases. Jung et al. [7] used the rate of increase together with delayed distribution estimation and statistical induction to establish a mathematical model, based on COVID-2019 case data reported before January 24. The predicted cumulative number of confirmed cases for up until January 24 was 6,924, and the predicted death ratio was 5.3%; these figures were within the 95% confidence interval. Compared with previous methods for establishing mathematical models, Fan et al. [8] adopted a statistical method for predicting the floating population in Wuhan City. The experiment indicated that the floating population in Wuhan region is highly correlated with the number of daily confirmed cases. The residence time of the floating population for local cases was longer than that for non-local cases, which results in a lower predicted number of confirmed cases in the areas around Hubei Province. The prediction results indicate that approximately 80% of the epidemic will be centralized in the top 30 districts.

However, applications of deep learning methods have mainly used the genome of the 2019-cCoV virus to predict disease propagation. Yang et al. [9] used the Susceptible-Exposed-Infectious-Removed model to integrate the epidemic curve, combining it with the long short-term memory model. The maximum value was reached on February 28, and the curve gradually lowered in late April. Hu et al. [10] used an improved stacked autoencoder and a cluster algorithm to group the instantaneous confirmed cases in every province; they noted a high accuracy in AI-based methods for COVID-19 trajectory prediction. The epidemic was predicted to end in mid-April. Guo et al. [11] used deep learning–based virus host prediction to compare the gene sequence of 2019-nCoVs with those of Severe Acute Respiratory Syndrome Coronavirus (SARS-CoV), bat SARS corona virus, and Middle East respiratory syndrome–related coronavirus (MERS-CoV). The bat SARS coronavirus was discovered to have a more similar mode of infection to COVID-19. Metsky et al. [12] used a nucleic acid

test based on clustered regularly interspaced short palindromic repeats (CRISPR) genome editing and selected 67 viruses and subspecies as well as subspecies that are highly similar to 2019-nCoV. Thus, 67 test methods were designed in the ADAPT system to increase the sensitivity and speed of virus detection.

Riou et al. [13] simulated the early outbreak trajectories of 2019-nCoV and noted that the basic reproduction number R of 2019-nCoV was approximately 2.2 (90% high density interval 1.4–3.8) and that 2019-nCoV has the potential for continual infection between people. Liu et al. [14] compared 2019-nCoV with SARS and estimated the doubling time of 2019-nCoV and SARS as well as the basic reproduction number r_0 and time-varying instantaneous reproduction number r_t through data analysis. They discovered that the infectivity of 2019-nCoV may be stronger than SARS, but that disease control efforts are effective. Ming et al. [15] adopted an improved version of the Susceptible-Infectious-Recovered (SIR) model to predict the actual number of infection cases of 2019-nCoV as well as the actual load on the intensive care units under different diagnosis rates and public health intervention efficacies. They discovered that under a 50% diagnosis rate and no public health intervention, the actual number of cases will be significantly higher than the reported number, whereas under a 70% public health intervention, the load on the health system will decrease substantially. Zhao et al. [16] used a probability prediction model to accurately predict the infection nodes from snapshots of spreading. Fountain-Jones et al. [17] used machine learning to establish pathogen-risk models and compared the prediction results of different machine learning methods and explained the results by using game theory.

Benvenuto et al. [18] adopted an autoregressive integrated moving average model to predict the epidemic trend and morbidity of 2019-nCoV with a 95% confidence interval. They discovered that if the virus does not mutate, the case number will reach a plateau. Li et al. [19] used a function to separately describe the daily infection and death data of 2019-nCoV in Hubei and outside Hubei. The author thought that the inflection point in the Hubei region was at February 6, 2020, and that the epidemic will end on March 10, 2020, with an estimated infection rate of 39,000 people. However, the data did not include the data after February 12, where such inclusion will increase the predicted figures by 1.4 times. Yang et al. [9] described the clinical characteristics and imaging manifestation of the infected cases of COVID-19 that had been confirmed in the hospitals in Wenzhou area. In addition, the patients with and without travel or residence history in Hubei were compared. Tian et al. [20] analyzed the clinical and epidemiological characteristics of COVID-19 in the Beijing area. The characteristics of severe confirmed cases and common confirmed cases were compared, and the characteristics of COVID-19 and SARS were compared as well. Chen et al. [21] analyzed some cases of pregnant women with COVID-19 and noted no evidence that COVID-19 causes intrauterine infection through vertical transmission among women in late pregnancy. The major contribution of that study is its fast establishment of a prediction model by using deep learning with a small dataset, making it an important reference for other countries in their containment of the COVID-19 epidemic.

The structure of this study proceeds as follows. The first section introduces the entire study. The second section is a literature review. The following third section details this study's proposed deep neural network algorithm. The fourth section presents and discusses the experiment results in detail. Finally, the fifth section concludes the entire study and underscores the contribution of this study and the predicted trend of the COVID-19 epidemic.

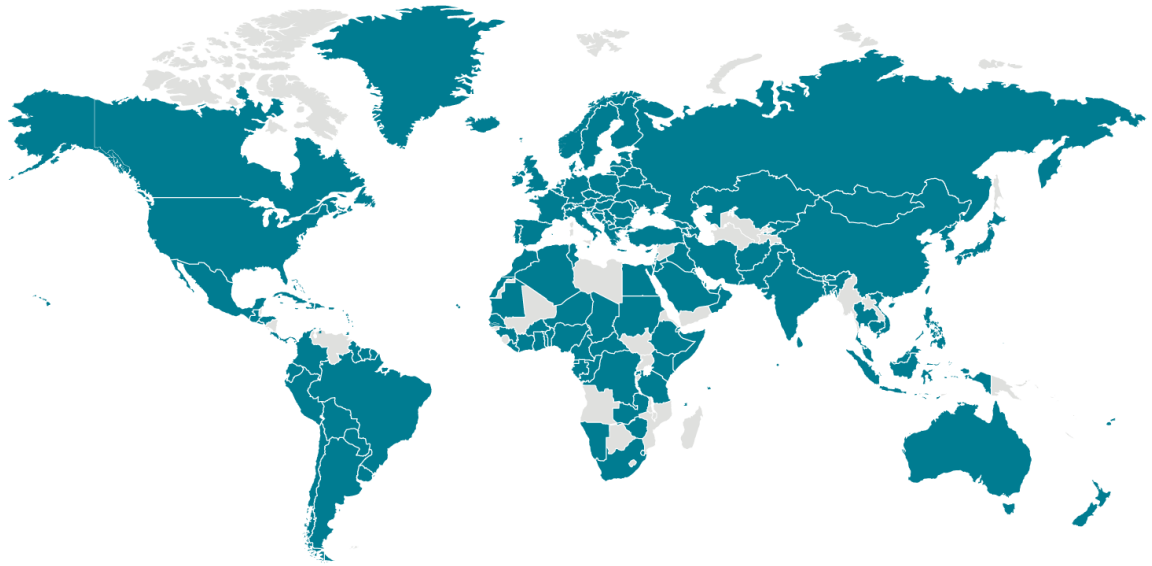

Fig. 1. Global Map of Confirmed COVID-19 Cases as of 12:00 a.m. ET, March 21, 2020 [2].

3. Artificial neural networks: A background

An Artificial Neural Network (ANN) [22, 23] is a mathematical model that mimics how neurons operate in organisms. It is a very powerful tool for establishing nonlinear models. An early ANN structure is the Multilayer Perceptron (MLP), which uses the neural network of fully connected structures; it has decent efficacy and numerous applications. However, if the data is too complex, simply using the MLP structure may cause the model to be unable to effectively learn how to handle every situation. At present, ANN has already developed into various new structures. The main structure of this study is the Convolutional Neural Network (CNN) [24, 25], and three other neural network structures are compared with it. These four neural network structures are detailed in the following subsections.

3.1. Convolutional neural network

The 1D convolution operation [26] is illustrated in Fig. 2. The difference between CNN and MLP is that CNN uses the concept of weight sharing. As illustrated in Fig. 2, the advantage of CNN is that its weight number does not have to be as large as that for a fully connected structure. Consequently, the training is relatively easier, and important characteristics are extracted more effectively. CNN is a feedforward neural network, which is an improvement from MLP. CNN contains four levels in structure: an input layer, convolutional layer, pooling layer, and fully connected layer.

The deep CNN structure proposed in this study is illustrated in Fig. 2, and the structure is composed of CNN and the dropout layer. The input layer structure is constituted by six time sequences composed of factors influencing the cumulative number of cases. The convolutional layer structure is divided into four layers, and each convolution layer has 16, 32, 32, and 64 convolutional kernels. Going through every convolutional layer, the convolutional kernels of the previous layer slide in the input data matrixes. The convolution process can be expressed in Equation (1), in which $\boldsymbol{X}_{ij}$ is the *i*th and *j*th matrix in the row and column direction, respectively, corresponding to the convolution kernels in the input matrix through smooth shifting. *K* is the convolution kernel, and $\boldsymbol{\gamma}$ is the output matrix.

$$\boldsymbol{\gamma}(i,j) = \boldsymbol{X}_{ij} * \boldsymbol{K} \tag{1}$$

The structure principle of the fully connected layer can be expressed by Equation (2):

$$\boldsymbol{o} = f\left(\boldsymbol{w}_f^T \boldsymbol{x} + \boldsymbol{b}\right) \tag{2}$$

In (2), $\boldsymbol{o}$ is the vector composed of output values, $\boldsymbol{x}$ is the vector composed of input values, $\boldsymbol{w}_f^T$ is the vector composed of weight values, $\boldsymbol{b}$ is the vector composed of threshold values, and f is the activation function. The output of the convolution layer can yield a 1D vector through Flatten expansion. Subsequently, the vectors are connected to the fully connected layer (dense) to obtain a 1D output. At the time of writing, the

COVID-19 epidemic has continued for only 3 months, 1 week, and 3 days. Thus, considering the small number of obtained samples, this model prevents overfitting by introducing the method of dropout regularization.

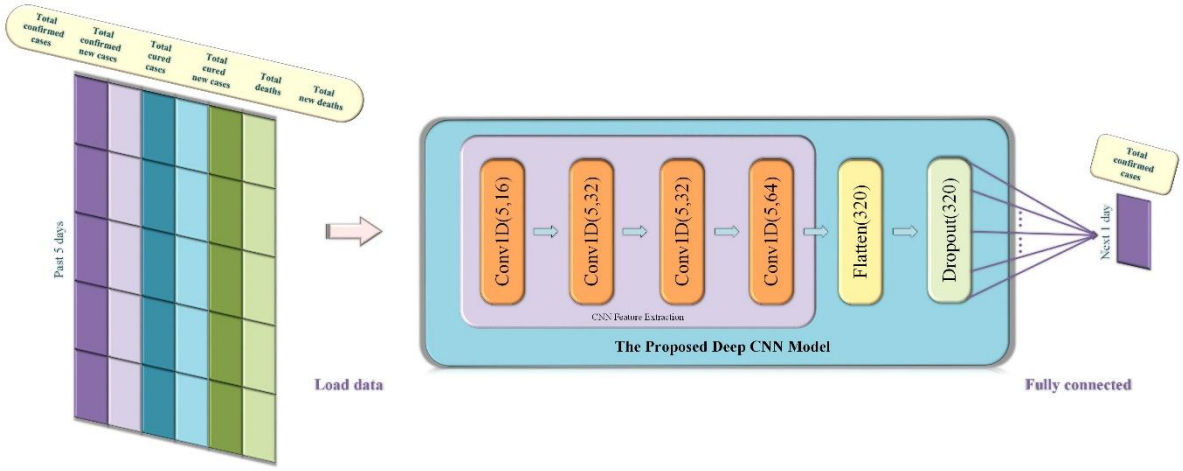

Fig. 2. Structure of the proposed deep CNN model.

3.2. Multilayer perceptron

A MLP is an ANN model that includes the input layer, hidden layer, and output layer. The structure of the ANN is illustrated in Fig. 3. Different connection layers are all fully connected, and the principle is similar to that of MLP. Each neural unit is connected with a weight coefficient (w_i), and the combination of transmission result $w_i x_i$ and the deviation b_i is calculated using Equation (3). In addition, current neural unit output results are obtained through the activation function f.

$$y_i = f(w_i x_i + b_i) \tag{3}$$

The structure of the proposed deep MLP is illustrated in Fig. 3. The structure is composed of two levels of MLP, and each MLP layer has 16 neural units. The input structure is constituted by six factors influencing the cumulative number of cases, with the time step of 5. Through a Flatten expansion, a 1×30 vector is derived, and the output is obtained after connecting the vector to the fully connected layer (dense).

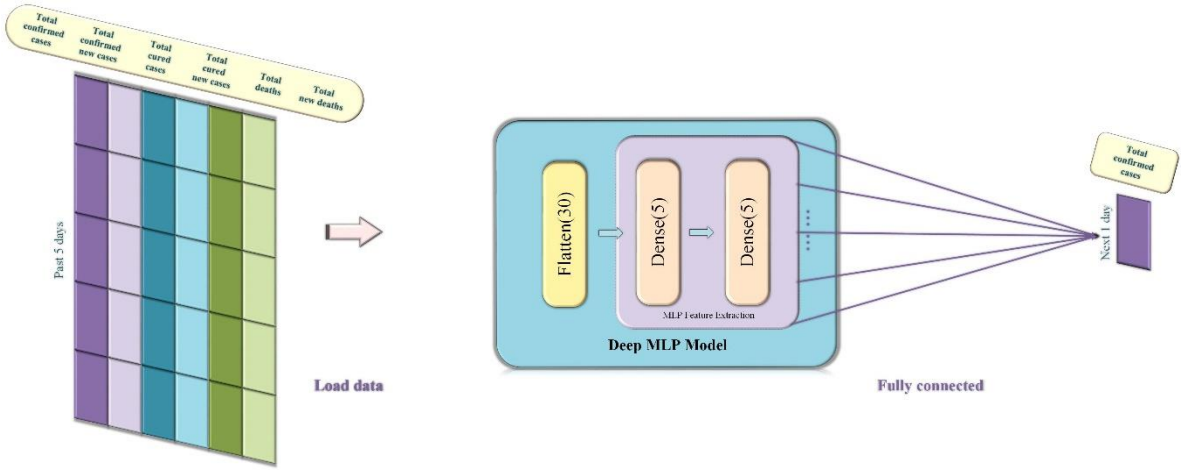

Fig. 3. Structure of the comparative deep neural network MLP adopted in this study.

3.3. Long short-term memory neural network

The long short-term memory model (LSTM) [27, 28] is an improvement from the recurrent neural network. The difference between the RNN and LSTM is that for LSTM, a cell state is added to store long-term states. In the neural unit model structure in Fig. 4 (a), the internal structure of LSTM can be divided into the input gate, forget gate, and output gate. The principle of the LSTM input gate is expressed in the following formulae.

Equation (4) is used to decide which piece of information is to be added by passing h_{t-1} and x_t through the sigmoid layer. Subsequently, Equation (5) is used to pass h_{t-1} and x_t through the tanh layer to obtain new information $\tilde{C}_t$. Equation (6) is used to combine the information of the current moment $\tilde{C}_t$ and long-term memory C_{t-1} into a new memory state C_t.

$$i_t = \sigma(W_i \cdot [h_{t-1}, x_t] + b_i) \quad (4)$$

$$\tilde{C}_t = \tanh(W_c \cdot [h_{t-1}, x_t] + b_c) \quad (5)$$

$$C_t = f_t C_{t-1} + i_t \tilde{C}_t \quad (6)$$

The forget gate of the LSTM uses a sigmoid layer and a dot product to allow information to pass through selectively. Equation (7) allows the LSTM to decide whether to forget the related information of the previous cell, at a certain probability, in which W_f is the weight matrix, and b_f is the offset term.

$$f_t = \sigma\left(W_f \cdot [h_{t-1}, x_t] + b_f\right) \quad (7)$$

The output gate of LSTM decides which states are required to be maintained by the input h_{t-1} and x_t according to Equations (8) and (9). The final output results are obtained by passing the new information C_t through the tanh layer to multiply with state judgement vectors.

$$O_t = \sigma(W_O \cdot [h_{t-1}, x_t] + b_O) \quad (8)$$

$$h_t = O_t \tanh(C_t) \quad (9)$$

The deep LSTM structure proposed in this study is illustrated in Fig. 4 (b). The structure is composed of two LSTM layers, and each layer has 16 neural units. The input structure is constituted by six factors influencing the cumulative number of cases, with a time step of 5. A 1D output is obtained through the fully connected layer.

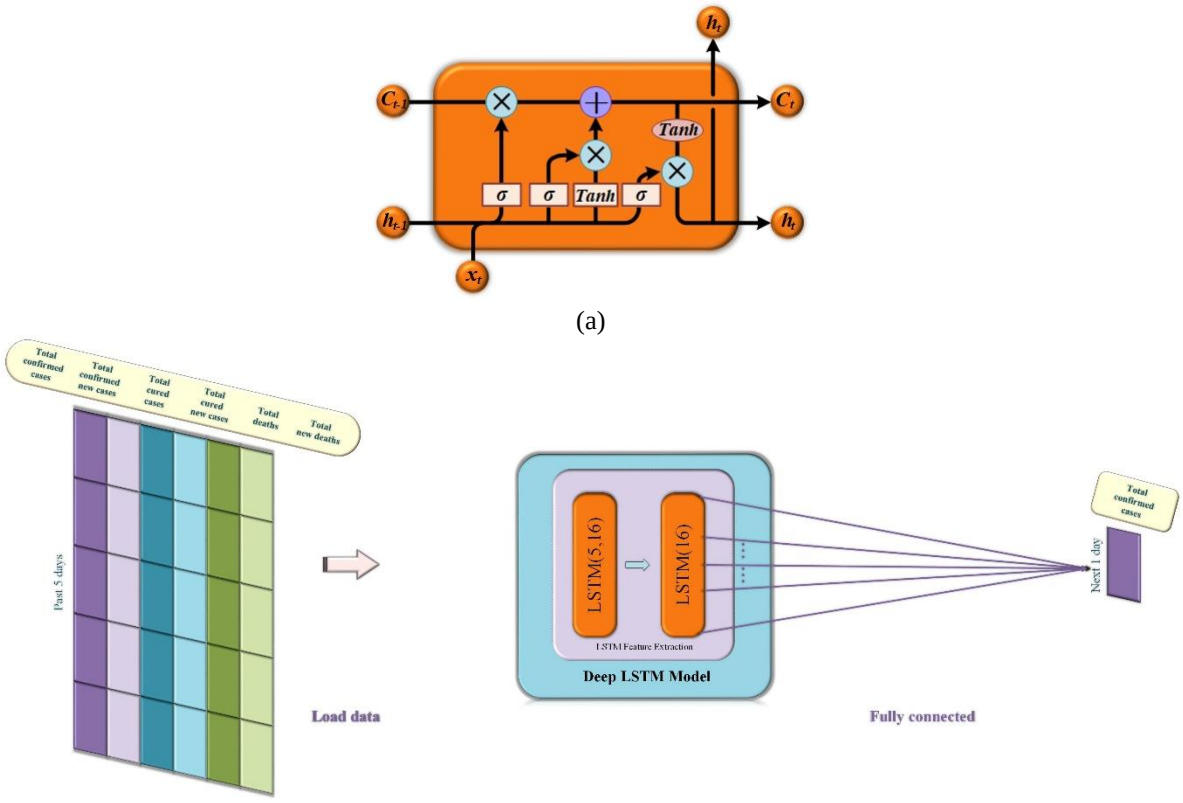

Fig. 4. Structure of the comparative deep neural network LSTM adopted in this study. (a) LSTM neural unit; (b) the deep neural network LSTM model with an input layer consisting six input signals.

3.4. Gate recurrent unit

The Gate Recurrent Unit (GRU) [29, 30] is a variation of the LSTM, as illustrated in Fig. 5 (a). GRU changes the input gate and forget gate of LSTM into the update gate. GRU retains the effect of LSTM and simplifies the internal structure of GRU model units. The principle of GRU's update gate is described in Equation (10). Specifically, the neural unit information of the previous moment h_{t-1} and the input data of the

current moment x_t are combined and input to the sigmoid layer to obtain the update information of the current moment z_t. W is the weight matrix.

$$z_t = \sigma(W_z \cdot [h_{t-1}, x_t]) \quad (10)$$

The principle of the GRU reset gate is described in Equation (11). The reset information r_t is reserved after h_{t-1} and x_t are separately combined with the weight matrix.

$$r_t = \sigma(W_r \cdot [h_{t-1}, x_t]) \quad (11)$$

The input information of the current moment x_t is maintained with the obtained r_t at the weight probability. The following Formula (12) is used to calculate the information of the current moment $\tilde{h}_t$.

$$\tilde{h}_t = \tanh(W \cdot [r_t * h_{t-1}, x_t]) \quad (12)$$

Equation (13) combines the reserved long-term memory z_t and the information of the current moment $\tilde{h}_t$ to obtain new information h_t.

$$h_t = (1 - z_t)\, h_{t-1} + z_t\, \tilde{h}_t \quad (13)$$

The structure of the proposed deep GRU is shown in Fig. 5 (b). The structure is composed of two GRU layers, and each layer has 16 neural units. The input structure is constituted by six factors influencing the cumulative number of cases, with a time step of 5. A 1D output is obtained through the fully connected layer.

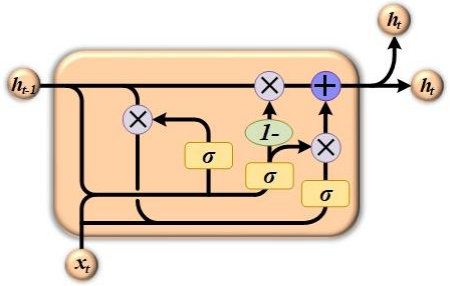

(**a**)

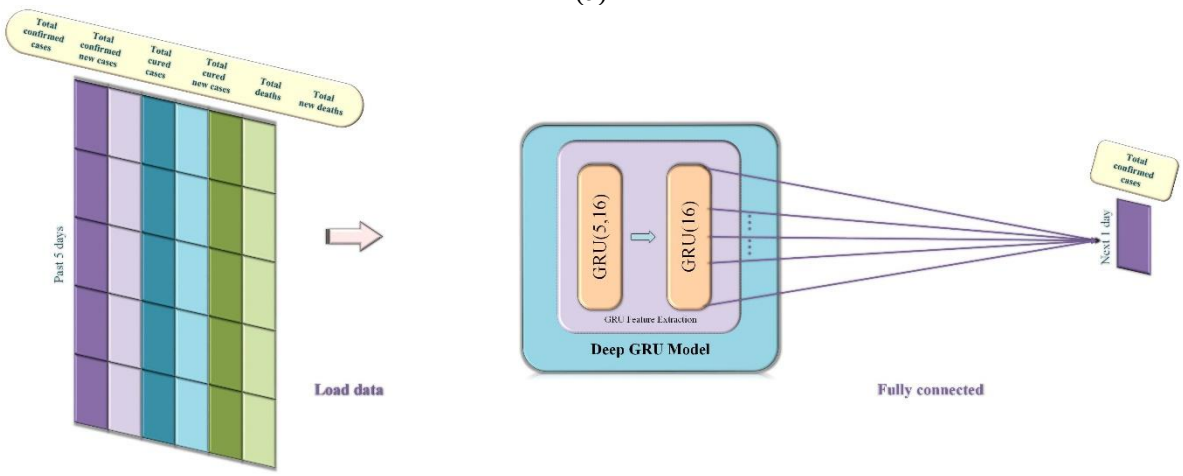

(**b**)

Fig. 5. Structure of the comparative deep neural network GRU adopted in this study. (a) GRU neural unit; (b) the deep neural network GRU model with an input layer consisting six input signals.

The pseudocode of the proposed CNN is described in Algorithm 1. Specifically, the dataset and test set are first loaded. The input data are then reconstructed into 3D matrixes, and the output data format is set to the 2D matrix. The CNN model is constructed, and related CNN parameters are set. Before the training starts, the weighting value w is initialized, and the repeat operator a is initialized as 0. In the training process, the training samples are trained in batches, and the loss function is calculated once per batch to update the weight value w. After the training, the test set data are registered to the trained network. The errors are calculated, and the actual values and error values are compared.

Algorithm 1 Convolutional Neural Network

Input, target, and hyperparameter setting:

Load the training set and testing set.

Reshape the input into the corresponding three-dimensional matrix.

1. The first dimension is the sample index.
2. The second dimension is the time step.
3. The third dimension is the characteristic.

Reshape the output into a two-dimensional matrix.

1. The first dimension is the sample target index.
2. The second dimension is the sample target.

Set relevant parameters of the CNN model.

Training:

Initialize the weight w

$s \rightarrow$ Total number of training set samples

$c \rightarrow$ Batch size

$a \rightarrow 0$

for i to epoch then

for k to s then

$j = k \bmod c$

if $j = 0$ then

$j = \mathbf{c}$

end

if $j - a > 0$ then

Calculate the output using Equations (1) and (2) for training set samples in the batch.

else

Calculate the loss using loss function, update the weight using optimizer, and calculate the output using Equations (1) and (2) for training set samples in the next batch.

end

$a = j$

end

end

Testing:

The established CNN model is used to predict the testing set. The real value is compared with the predicted value, and the prediction error is calculated.

4. Experimental Results and Discussion

Data on confirmed cases of COVID-19 from January 23, 2020 to March 2, 2020, and from January 23, 2020 to March 2, 2020, were obtained from Surging News Network (a media outlet) [9] and WHO [31], respectively. In this experiment, the two evaluation indexes of the mean absolute error (MAE) and root mean square error (RMSE) were used; their formulae are presented in Equations (14) and (15). To conduct comprehensive efficacy tests, the dataset for January 23 to February 17 was chosen as the training data, and the dataset for February 18 to March 2 was used as testing data. Figs. 6 to 12 present the comparative prediction results of all the algorithms. The detailed MAE and RMSE values are listed in Tables I, II, III, and IV. The

experiment results indicated that the GRU has decent efficacy, and that CNN is the best performing algorithm among its counterparts tested. The experiment demonstrated that the characteristic extraction of CNN is very helpful for predicting the number of confirmed cases of COVID-19.

$$\mathrm{MAE} = \frac{1}{N}\sum_{n=1}^{N}\left|y_n - \hat{y}_n\right| \tag{14}$$

$$\mathrm{RMSE} = \sqrt{\frac{\sum_{n=1}^{N}\left(y_n - \hat{y}_n\right)^2}{N}} \tag{15}$$

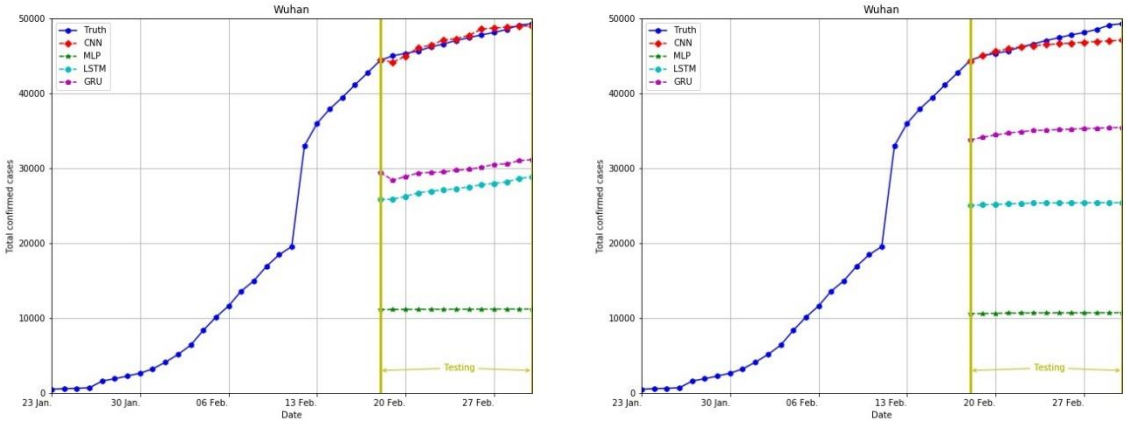

(**a**) (**b**)

Fig. 6. Comparison of prediction results for the cumulative number of confirmed cases in Wuhan City, Hubei Province, China. The comparison used the deep neural networks CNN, MLP, LSTM, and GRU. (a) Six important factors were adopted as the input layer: new confirmed cases, new deceased cases, new cured cases, cumulative confirmed cases, cumulative deceased cases, and cumulative cured cases. (b) Only one important factor was adopted as the input layer: cumulative confirmed cases.

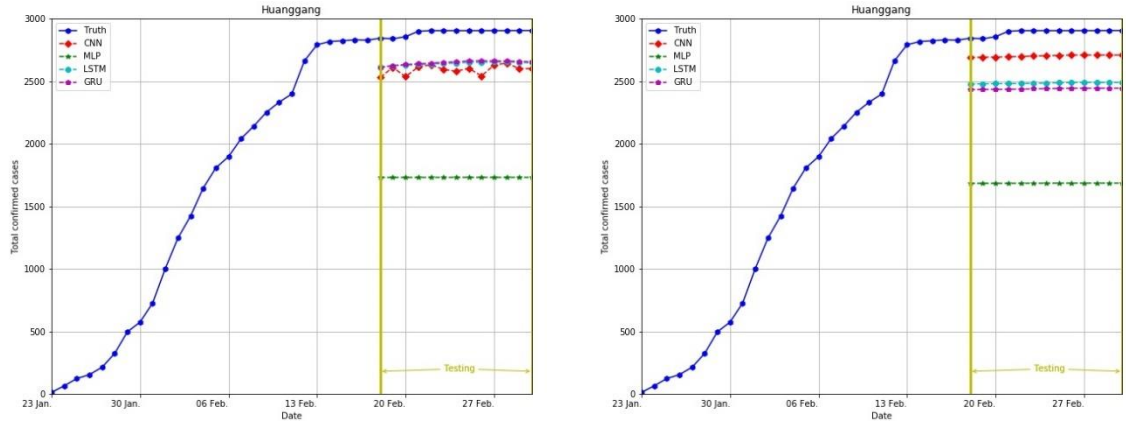

(**a**) (**b**)

Fig. 7. Comparison of prediction results for the cumulative number of confirmed cases in Huanggang City, Hubei Province, China. The comparison used the deep neural networks CNN, MLP, LSTM, and GRU. (a) Six important factors were adopted as the input layer: new confirmed cases, new deceased cases, new cured cases, cumulative confirmed cases, cumulative deceased cases, and cumulative cured cases. (b) Only one important factor was adopted as the input layer: cumulative confirmed cases.

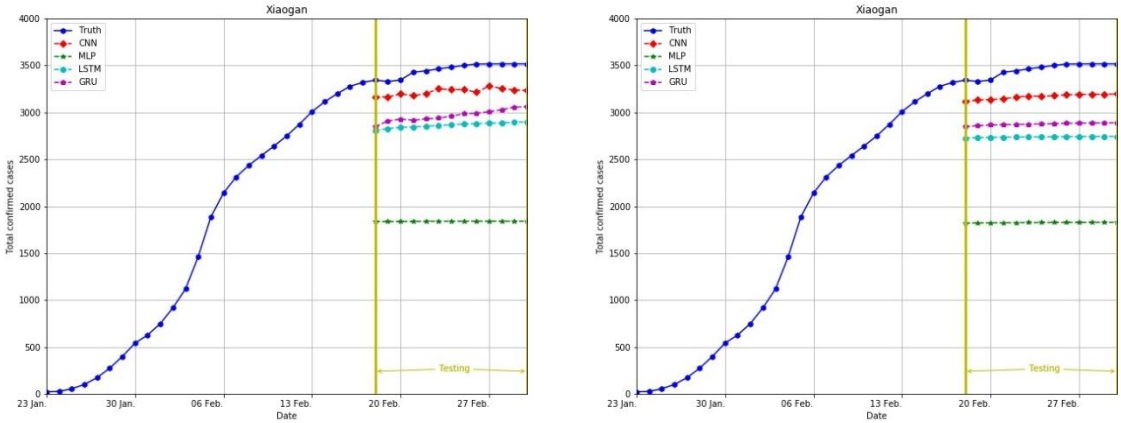

(**a**) (**b**)

Fig. 8. Comparison of prediction results for the cumulative number of confirmed cases in Xiaogan City, Hubei Province, China. The comparison used the deep neural networks CNN, MLP, LSTM, and GRU. (a) Six important factors were adopted as the input layer: new confirmed cases, new deceased cases, new cured cases, cumulative confirmed cases, cumulative deceased cases, and cumulative cured cases. (b) Only one important factor was adopted as the input layer: cumulative confirmed cases.

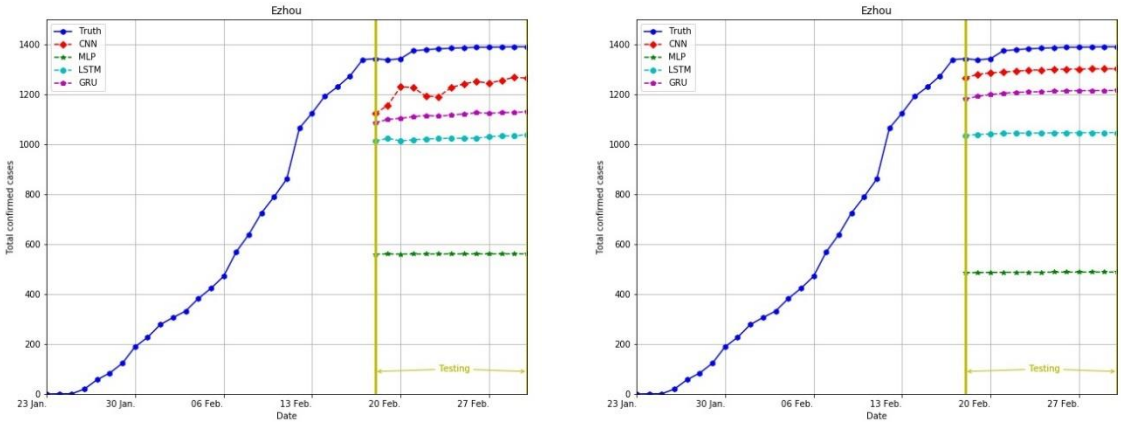

(**a**) (**b**)

Fig. 9. Comparison of prediction results for the cumulative number of confirmed cases in Ezhou City, Hubei Province, China. The comparison used the deep neural networks CNN, MLP, LSTM, and GRU. (a) Six important factors were adopted as the input layer: new confirmed cases, new deceased cases, new cured cases, cumulative confirmed cases, cumulative deceased cases, and cumulative cured cases. (b) Only one important factor was adopted as the input layer: cumulative confirmed cases.

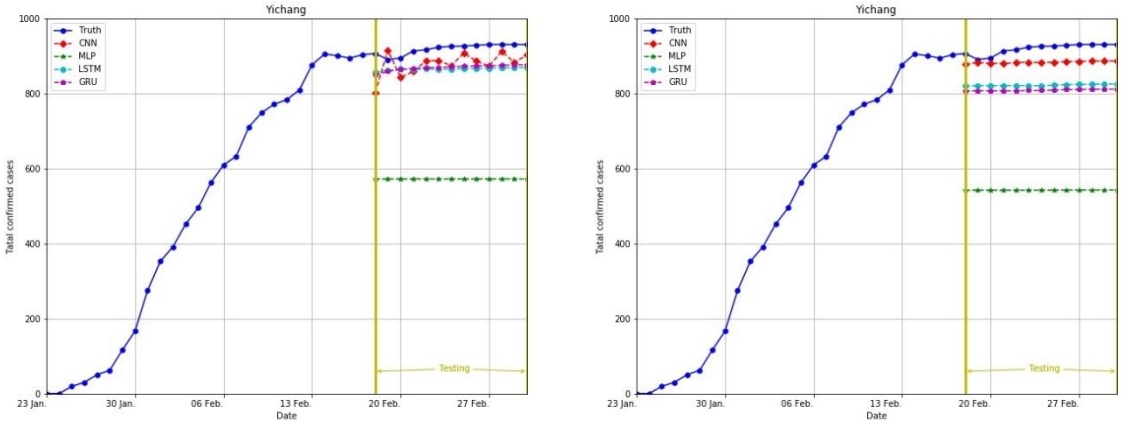

Fig. 10. Comparison of prediction results for the cumulative number of confirmed cases in Yichang City, Hubei Province, China. The comparison used the deep neural networks CNN, MLP, LSTM, and GRU. (a) Six important factors were adopted as the input layer: new confirmed cases, new deceased cases, new cured cases, cumulative confirmed cases, cumulative deceased cases, and cumulative cured cases. (b) Only one important factor was adopted as the input layer: cumulative confirmed cases.

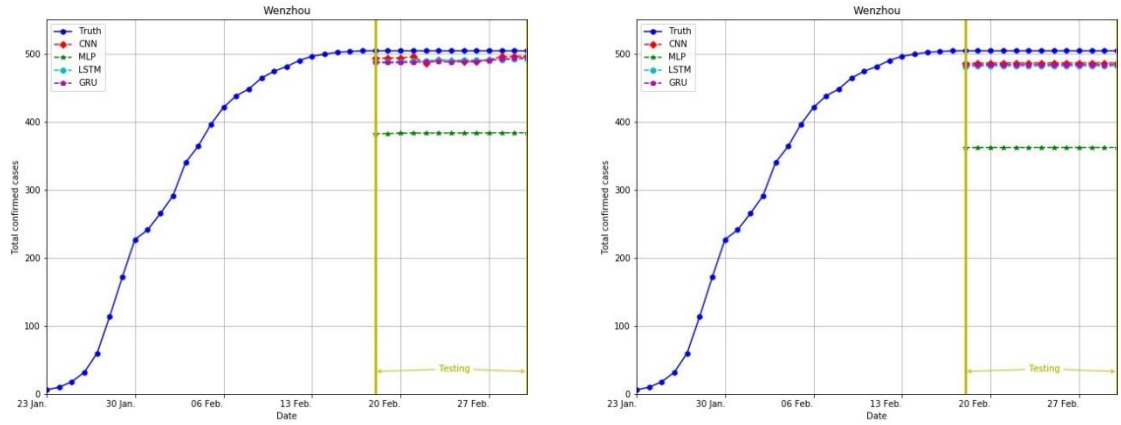

Fig. 11. Comparison of prediction results for the cumulative number of confirmed cases in Wenzhou City, Zhejiang Province, China. The comparison used the deep neural networks CNN, MLP, LSTM, and GRU. (a) Six important factors were adopted as the input layer: new confirmed cases, new deceased cases, new cured cases, cumulative confirmed cases, cumulative deceased cases, and cumulative cured cases. (b) Only one important factor was adopted as the input layer: cumulative confirmed cases.

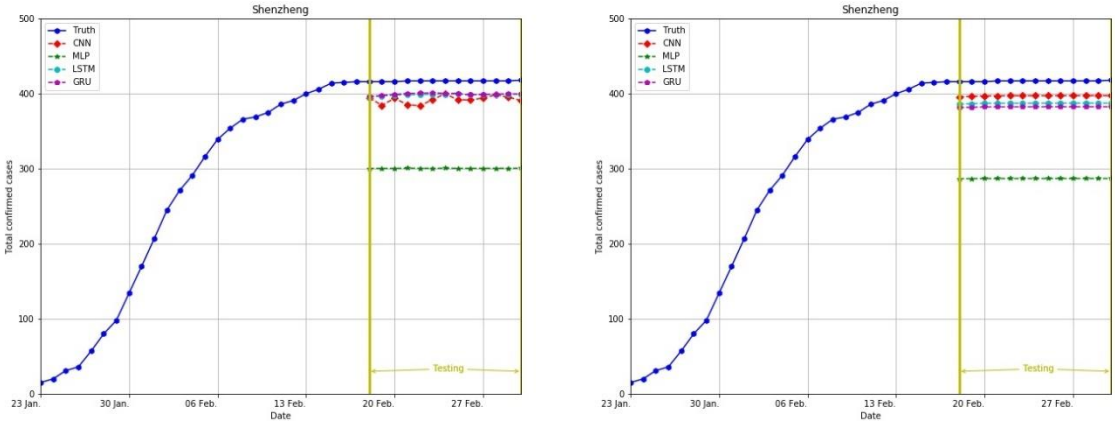

(**a**) (**b**)

Fig. 12. Comparison of prediction results for the cumulative number of confirmed cases in Shenzhen City, Guangdong Province, China. The comparison used the deep neural networks CNN, MLP, LSTM, and GRU. (a) Six important factors were adopted as the input layer: new confirmed cases, new deceased cases, new cured cases, cumulative confirmed cases, cumulative deceased cases, and cumulative cured cases. (b) Only one important factor was adopted as the input layer: cumulative confirmed cases.

TABLE I

EXPERIMENTAL RESULTS IN TERMS OF MEAN ABSOLUTE ERROR OF THE INPUT LAYER OF SIX NEURONS

City	GRU	LSTM	MLP	CNN
Wuhan	17119.101	19671.849	35797.372	**426.179**
Huanggang	243.399	250.142	1159.923	**89.026**
Xiaogan	489.004	592.220	1616.017	**87.343**
Ezhou	259.843	350.798	814.801	**77.942**
Yichang	50.219	53.632	346.853	**31.688**
Wenzhou	15.067	13.988	120.844	**4.617**
Shenzhen	17.414	18.200	116.240	**3.808**
Avg.	2599.150	2992.976	5710.293	**102.943**

TABLE II

EXPERIMENTAL RESULTS IN TERMS OF MEAN ABSOLUTE ERROR OF THE INPUT LAYER OF A SINGLE NEURON

City	GRU	LSTM	MLP	CNN
Wuhan	12054.218	21669.078	36307.670	**1131.627**
Huanggang	450.634	405.468	1206.190	**255.561**
Xiaogan	580.525	717.547	1629.771	**389.392**
Ezhou	168.118	331.491	887.933	**102.507**
Yichang	109.966	96.664	376.636	**63.651**
Wenzhou	**20.417**	22.303	141.863	22.138
Shenzhen	34.452	29.589	129.942	**27.136**
Avg.	1916.904	3324.591	5811.429	**284.573**

TABLE III

EXPERIMENTAL RESULTS IN TERMS OF ROOT MEAN SQUARE ERROR OF THE INPUT LAYER OF SIX NEURONS

City	GRU	LSTM	MLP	CNN
Wuhan	17140.879	19681.133	35829.022	**456.910**
Huanggang	243.715	250.594	1160.173	**94.271**
Xiaogan	490.381	593.989	1617.454	**90.685**
Ezhou	260.019	351.126	815.025	**81.469**
Yichang	50.960	54.844	347.112	**32.855**
Wenzhou	15.264	14.051	120.845	**5.106**
Shenzhen	17.446	18.217	116.241	**4.779**
Avg.	2602.666	2994.851	5715.125	**109.439**

TABLE IV

EXPERIMENTAL RESULTS IN TERMS OF ROOT MEAN SQUARE ERROR OF THE INPUT LAYER OF A SINGLE NEURON

City	GRU	LSTM	MLP	CNN
Wuhan	12101.919	21715.728	36338.153	**1416.082**
Huanggang	451.136	406.029	1206.424	**256.246**
Xiaogan	583.509	720.488	1631.175	**391.768**
Ezhou	168.461	331.896	888.127	**102.974**
Yichang	110.629	97.439	376.867	**64.649**
Wenzhou	20.417	22.303	141.863	**22.139**
Shenzhen	34.454	29.591	129.943	**27.139**
Avg.	1924.361	3331.925	5816.079	**325.857**

Regarding the deep neural network prediction results for six and one-input factors, the MAE and RMSE values are listed in Tables 1 to 4. The MAE results from low to high are as follows: CNN (102.943, 284.573), GRU (2599.150, 1916.904), LSTM (2992.976, 3324.591), and MLP (5710.293, 5811.429). The RMSE results from low to high are as follows: CNN (109.439, 325.857), GRU (2602.666, 1924.361), LSTM (2994.851, 3331.925), and MLP (5715.125, 5816.079). The experiment results demonstrated that GRU and LSTM have decent efficacies and that CNN had the best performance. This experiment also demonstrated that the procedure of initial characteristic extraction through CNN and the subsequent input of characteristic values to the CNN structure greatly aid the prediction of the cumulative number of confirmed cases of COVID-19.

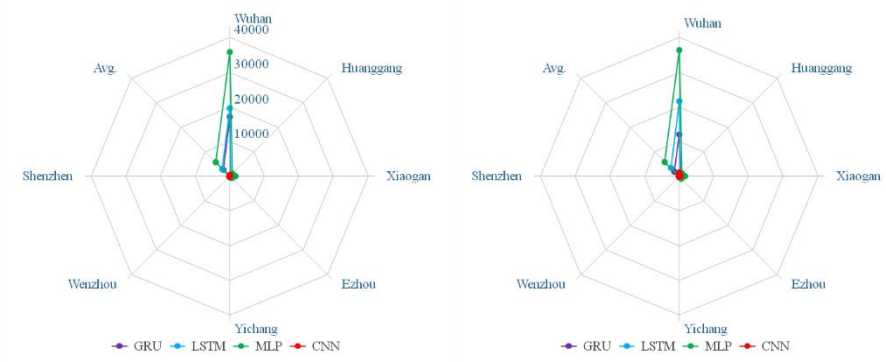

(**a**) (**b**)

Fig. 13. MAE radar charts. (a) Six factors were adopted as the input layer. (b) Only one factor was adopted as the input layer.

Fig. 13 (a) and (b) presents the radar charts of MAE values for the comparison between the output results and real values for six and one factors, respectively. Regardless of whether one or six factors were used, the prediction results, in terms of MAE, of the proposed CNN model were superior to those of its counterparts. For the proposed CNN model, the use of six factors yielded better prediction results, in terms of MAE, in comparison to the use of only one factor, particularly for Wuhan City.

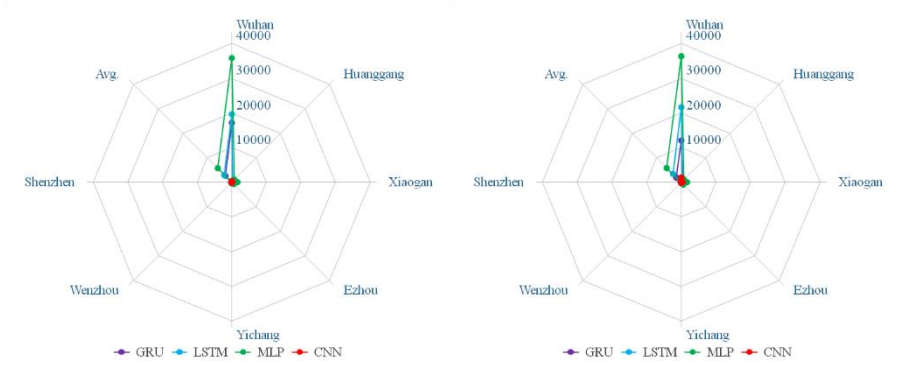

(a) **(b)**

Fig. 14. RMSE radar charts. (a) Six pieces of important information were adopted as the input layer. (b) Only one piece of information was adopted as the input layer.

Fig. 14 (a) and (b) presents the radar charts of RMSE values for the comparison between the output results and real values for six and one factors, respectively. The results further demonstrated the excellent predictive performance of the proposed CNN model for the cumulative number of confirmed cases of COVID-19, making the model a valuable reference for other countries in their establishment of country-specific COVID-19 prediction models. In general, the prediction performances of the models from most favorable to least favorable were those for CNN, GRU, LSTM, and MLP.

5. Conclusions

A novel and multi-input CNN deep neural network model was proposed in this study to predict the cumulative number of confirmed cases of COVID-19. The cumulative number of confirmed cases in the next day is predicted according to the previous five days' total number of confirmed cases, total confirmed new cases, total cured cases, total cured new cases, total deaths, and total new deaths. In the experiment, the datasets of those seven Chinese cities with severe confirmed cases—from Hubei Province, Guangdong Province, and Zhejiang Province—were used for the models' training and prediction. Because the COVID-19 epidemic is ongoing, the algorithm proposed in this study can rapidly use small datasets to establish models with high predictive accuracy, different from many other studies. In addition, with the algorithm, a deep learning network prediction model for the number of confirmed cases of COVID-19 was established, and the verification and comparison were conducted among different deep learning algorithms. The accuracy and reliability of the deep learning algorithm were verified by having it predict the future trend of COVID-19. Furthermore, experiments for multiple cities with more severe confirmed cases in China indicated that the prediction model of this study had the lowest error rate among its counterparts tested. However, at the time of writing, countries other than China have had COVID-19 outbreaks, such as Italy, South Korea, Iran, Spain, France, and Germany. In the future, the establishment of more complete databases will lead to improvements to the proposed prediction model. For example, deep learning networks with a mixed structure can be introduced to establish more accurate models, which can be applied to more countries. The predicted trends can aid the containment of the COVID-19 epidemic and extend the scope of application of artificial intelligence.

References

1. Zhu, N.; Zhang, D.; Wang, W.; Li, X.; Yang, B.; Song, J.; Zhao, X.; Huang, B.; Shi, W.; Lu, R.; Niu, P.; Zhan, F.; Ma, X.; Wang, D.; Xu, W.; Wu, G.; Gao, G. F.; Tan, W.; China Novel Coronavirus, I.; Research,

T., A Novel Coronavirus from Patients with Pneumonia in China, 2019. *N Engl J Med* **2020,** 382, (8), 727-733.

2. Locations with Confirmed COVID-19 Cases Global Map Available online: https://www.cdc.gov/coronavirus/2019-ncov/locations-confirmed-cases.html.
3. Roosa, K.; Lee, Y.; Luo, R.; Kirpich, A.; Rothenberg, R.; Hyman, J. M.; Yan, P.; Chowell, G., Short-term Forecasts of the COVID-19 Epidemic in Guangdong and Zhejiang, China: February 13-23, 2020. *J Clin Med* **2020,** 9, (2).
4. Z. Liu, P. M., O. Seydi, G. Webb, Predicting the cumulative number of cases for the COVID-19 epidemic in China from early data. **2020**.
5. Boldog, P.; Tekeli, T.; Vizi, Z.; Dénes, A.; Bartha, F. A.; Röst, G., Risk Assessment of Novel Coronavirus COVID-19 Outbreaks Outside China. *Journal of Clinical Medicine* **2020,** 9, (2).
6. Al-Qaness, M. A. A.; Ewees, A. A.; Fan, H.; Abd El Aziz, M., Optimization Method for Forecasting Confirmed Cases of COVID-19 in China. *J Clin Med* **2020,** 9, (3).
7. Jung, S.-m.; Akhmetzhanov, A. R.; Hayashi, K.; Linton, N. M.; Yang, Y.; Yuan, B.; Kobayashi, T.; Kinoshita, R.; Nishiura, H., Real-Time Estimation of the Risk of Death from Novel Coronavirus (COVID-19) Infection: Inference Using Exported Cases. *Journal of Clinical Medicine* **2020,** 9, (2).
8. Fan, C.; Liu, L.; Guo, W.; Yang, A.; Ye, C.; Jilili, M.; Ren, M.; Xu, P.; Long, H.; Wang, Y., Prediction of Epidemic Spread of the 2019 Novel Coronavirus Driven by Spring Festival Transportation in China: A Population-Based Study. *Int J Environ Res Public Health* **2020,** 17, (5).
9. Yang, W.; Cao, Q.; Qin, L.; Wang, X.; Cheng, Z.; Pan, A.; Dai, J.; Sun, Q.; Zhao, F.; Qu, J.; Yan, F., Clinical characteristics and imaging manifestations of the 2019 novel coronavirus disease (COVID-19):A multi-center study in Wenzhou city, Zhejiang, China. *J Infect* **2020**.
10. Zixin Hu , Q. G., Shudi Li , Li Jin and Momiao Xiong Artificial Intelligence Forecasting of Covid-19 in China.
11. Guo, Q.; Li, M.; Wang, C.; Wang, P.; Fang, Z.; tan, J.; Wu, S.; Xiao, Y.; Zhu, H., Host and infectivity prediction of Wuhan 2019 novel coronavirus using deep learning algorithm. **2020**.
12. Metsky, H. C.; Freije, C. A.; Kosoko-Thoroddsen, T.-S. F.; Sabeti, P. C.; Myhrvold, C., CRISPR-based surveillance for COVID-19 using genomically-comprehensive machine learning design. **2020**.
13. Riou, J.; Althaus, C. L., PATTERN OF EARLY HUMAN-TO-HUMAN TRANSMISSION OF WUHAN 2019- NCOV. **2020**.
14. Liu, T.; Hu, J.; Xiao, J.; He, G.; Kang, M.; Rong, Z.; Lin, L.; Zhong, H.; Huang, Q.; Deng, A.; Zeng, W.; Tan, X.; Zeng, S.; Zhu, Z.; Li, J.; Gong, D.; Wan, D.; Chen, S.; Guo, L.; Li, Y.; Sun, L.; Liang, W.; Song, T.; He, J.; Ma, W., Time-varying transmission dynamics of Novel Coronavirus Pneumonia in China. **2020**.
15. Ming, W.-K.; Huang, J.; Zhang, C. J. P., Breaking down of healthcare system: Mathematical modelling for controlling the novel coronavirus (2019-nCoV) outbreak in Wuhan, China. **2020**.
16. Zhao, N.; Wang, J.; Yu, Y.; Zhao, J.-Y.; Chen, D.-B., Spreading predictability in complex networks. **2020**.
17. Fountain-Jones, N.; Machado, G.; Carver, S.; Packer, C.; Mendoza, M.; Craft, M. E., How to make more from exposure data? An integrated machine 1 learning pipeline to predict pathogen exposure **2019**.
18. Benvenuto, D.; Giovanetti, M.; Vassallo, L.; Angeletti, S.; Ciccozzi, M., Application of the ARIMA model on the COVID-2019 epidemic dataset. *Data in Brief* **2020,** 29.
19. Li, Q.; Feng, W.; Quan, Y. H., Trend and forecasting of the COVID-19 outbreak in China. *J Infect* **2020**.

20. Tian, S.; Hu, N.; Lou, J.; Chen, K.; Kang, X.; Xiang, Z.; Chen, H.; Wang, D.; Liu, N.; Liu, D.; Chen, G.; Zhang, Y.; Li, D.; Li, J.; Lian, H.; Niu, S.; Zhang, L.; Zhang, J., Characteristics of COVID-19 infection in Beijing. *J Infect* **2020**.
21. Chen, H.; Guo, J.; Wang, C.; Luo, F.; Yu, X.; Zhang, W.; Li, J.; Zhao, D.; Xu, D.; Gong, Q.; Liao, J.; Yang, H.; Hou, W.; Zhang, Y., Clinical characteristics and intrauterine vertical transmission potential of COVID-19 infection in nine pregnant women: a retrospective review of medical records. *The Lancet* **2020,** 395, (10226), 809-815.
22. Pham, T. A.; Ly, H.-B.; Tran, V. Q.; Giap, L. V.; Vu, H.-L. T.; Duong, H.-A. T., Prediction of Pile Axial Bearing Capacity Using Artificial Neural Network and Random Forest. *Applied Sciences* **2020,** 10, (5).
23. Khalid , Z.; Abbas , G.; Awais, M.; Alquthami, T.; Rasheed , M. B., A Novel Load Scheduling Mechanism Using Artificial Neural Network Based Customer Profiles in Smart Grid. *Energies* **2020,** 13, (5).
24. Wang, Y.; Li, Y.; Song, Y.; Rong, X., The Influence of the Activation Function in a Convolution Neural Network Model of Facial Expression Recognition. *Applied Sciences* **2020,** 10, (5).
25. Bai, T.; Pang, Y.; Wang, J.; Han, K.; Luo, J.; Wang, H.; Lin, J.; Wu, J.; Zhang, H., An Optimized Faster R-CNN Method Based on DRNet and RoI Align for Building Detection in Remote Sensing Images. *Remote Sensing* **2020,** 12, (5).
26. Abo-Tabik, M.; Costen, N.; Darby, J.; Benn, Y., Towards a Smart Smoking Cessation App: A 1D-CNN Model Predicting Smoking Events. *Sensors (Basel)* **2020,** 20, (4).
27. Zhang, Q.; Gao, T.; Liu, X.; Zheng, Y., Public Environment Emotion Prediction Model Using LSTM Network. *Sustainability* **2020,** 12, (4).
28. Zhang, M.; Geng, G.; Chen, J., Semi-Supervised Bidirectional Long Short-Term Memory and Conditional Random Fields Model for Named-Entity Recognition Using Embeddings from Language Models Representations. *Entropy* **2020,** 22, (2).
29. Jin, X. B.; Yang, N. X.; Wang, X. Y.; Bai, Y. T.; Su, T. L.; Kong, J. L., Hybrid Deep Learning Predictor for Smart Agriculture Sensing Based on Empirical Mode Decomposition and Gated Recurrent Unit Group Model. *Sensors (Basel)* **2020,** 20, (5).
30. Batur DİNler, Ö.; Aydin, N., An Optimal Feature Parameter Set Based on Gated Recurrent Unit Recurrent Neural Networks for Speech Segment Detection. *Applied Sciences* **2020,** 10, (4).
31. Coronavirus disease (COVID-2019) situation reports: http://www.who.int/emergencies/diseases/novel-coronavirus-2019/situation-reports.